Fast Fault Location Method for a Distribution System with High Penetration of PV

Miguel Jimenez Aparicio
Georgia Institute of Technology
maparicio6@gatech.edu

Santiago Grijalva
Georgia Institute of Technology
sgrijalva@ece.gatech.edu

Matthew J. Reno
Sandia National Laboratories
mjreno@sandia.gov

Abstract

Distribution systems with high levels of solar PV may experience notable changes due to external conditions, such as temperature or solar irradiation. Fault detection methods must be developed in order to support these changes of conditions. This paper develops a method for fast detection, location, and classification of faults in a system with a high level of solar PV. The method uses the Continuous Wavelet Transform (CWT) technique to detect the traveling waves produced by fault events. The CWT coefficients of the current waveform at the traveling wave arrival time provide a fingerprint that is characteristic of each fault type and location. Two Convolutional Neural Networks are trained to classify any new fault event. The method relays of several protection devices and doesn't require communication between them. The results show that for multiple fault scenarios and solar PV conditions, high accuracy for both location and type classification can be obtained.

1. Introduction

THE LOCATION of faults across a power system and the protection of electrical components have always been critical tasks in power engineering. In order to ensure the secure operation of the grid, many different monitoring and protection devices have been deployed across the system to detect and locate the presence of any faults in the shortest time possible, and to take the necessary actions to guarantee the safety of the rest of the system. If those actions are delayed, a fault could irreversibly damage a power device, and compromise the stability of the system in the most extreme cases.

According to [1], 80% of the interruptions in a distribution system are due to faults. The most probable causes are the contact between conductors or with the ground due to the wind, animals, or the breakdown of an electricity pole. Most of the faults occur on overhead lines [1]. However, other equipment, such as transformers or relays, could be involved as well. Energy quality and safety issues arise when a fault happens, posing a risk to both the equipment and human beings. Inevitably, a fault will lead to loss of power for the customers and to expensive repairs. Therein lies the importance of a fast and accurate fault location methods.

Over the last few years, there has been growing interest in distribution systems that include Distributed Generation (DGs), such as generators, energy storage, PV systems, and wind farms. The integration of these resources challenges the traditional techniques that have been used for fault location. Some techniques, such as those that depends on the variation of impedance, are no longer applicable since the structure of the distribution grid is no longer unidirectional [2]. Sources close to or at the load site can result in negative net demand, modifying the direction of the power flows. This is added to the fact that in transmission systems measuring devices can be located at each end of the line, but in distribution systems the large number of feeders makes widespread sensing impractical. All these factors contribute to increase the complexity of the already difficult task of fault location.

PV systems are being deployed in distribution systems at a rapid pace. Therefore, systems with a high penetration of solar PV are becoming more common and must be designed carefully. PV systems have different protection devices used to ensure the safety of the device against inner faults. However, external faults can still damage the system and therefore, any fault must be removed as fast as possible. The contributions of this paper are, first, a fault detection method that uses sudden magnitude differences in the coefficients of the Continuous Wavelet Transform (CWT) matrices of the current signals, along with a Deep Learning algorithm based on Convolutional Neural Networks (CNNs) which is employed to classify both fault location and type. Both tools, CNN and CWT, have been employed either independently or jointly in the literature for fault detection and classifications purposes, though the combination of this detection method, the signal processing stage and the obtained outcome of the classification algorithm makes this paper a valuable research.

URI: https://hdl.handle.net/10125/71005
978-0-9981331-4-0

The second contribution of this paper is to demonstrate that fault classification can be successfully accomplished on systems with high penetration of solar PV using the aforementioned method. For this purpose, fault signals under several PV conditions have been simulated. A case study on the IEEE 34 bus case has been prepared to draw conclusions.

The rest of the paper is structured as follows: In Section II some of the existing fault location techniques are discussed. The proposed method is presented in Section III. Simulation results are presented in Section IV. Finally, conclusions and ideas for a future work are presented in Sections V and VI.

2. Background

Techniques for fault location in distribution power systems are generally classified in three groups: first, monitoring and analyzing pre-fault and post-fault voltage and current phasors – or impedance-, second, traveling waves detection and examination, and, finally, Machine Learning techniques that can be applied to fault location.

The first group consists of techniques that are widely used for transmission systems, where voltage and current measurements are available for each line. When a fault occurs, there is a change in the X/R impedance ratio, which induces a phase shift between voltage and current. For example, in [3], this method is applied to determine the phases that are faulty.

The second group encompasses all the techniques related to the analysis of the propagated traveling waves produced by a fault. These high-frequency waves are reflected at the end of the lines. Some methods use the time differences between consecutive arrivals of the wave to calculate the distance to the fault [4]. Other methods such as [2] decompose the wave signal into decoupled modes and calculate the fault location based on the time lag between the arrival times of the different modes, knowing the propagation characteristics of each mode. All these methods generally use Continuous Wavelet Transform (CWT) or Discrete Wavelet Transform (DWT) to analyze the frequencies that form the signal and to determine the instant when the high-frequency wave arrives. Some studies such as [5] have improved the performance of the wavelet transform. According to this research, using an inferred mother wavelet from the traveling wave improves the detection of the frequency components, which can be characteristic of the path followed by the wave during the propagation [6].

The third group of techniques is composed by Machine Learning and other Artificial Intelligence algorithms that are employed for fault location. In the literature, the proposed methods generally belong to two categories: fault classifiers (type, section, resistance, etc.) and algorithms that seek to calculate the exact location of the fault. Regarding the first type, some studies propose methods to identify faults in many different lines. For example, [7] applies Fuzzy Logic to the CWT coefficients in order to determine the faulty phases, while [8] choses a Support Vector Machine (SVM). In the case of [9], a Multi-Layer Perceptron (MLP) Neural Network is proposed to obtain the fault resistance using the voltage and current values before and after the fault. However, the state-of-the-art classifiers use Convolutional Neural Networks (CNN), which is a powerful tool for extracting features. In [10], a CNN is trained to infer the faulty line in a distribution system. The dataset used for learning is just the CWT coefficient matrix of the transient zero-sequence current at each bus. It is claimed that this method is superior to other classifiers and it is resilient against several fault conditions and network changes. CNN can also be trained with 1-Dimensional arrays. For instance, in [11], the high-frequency components, extracted using Empirical Mode Decomposition, are used to obtain the faulty section of an HVDC transmission line. Another study [12] proposes an Adaptative Convolutional Neural Networks (ACNN) to infer the fault type in a transmission line using measurements from two Phasor Measurement Units (PMUs). It is stated that ACNN, in comparison to CNN, are trained faster and have a slightly better accuracy.

Regarding the algorithms that are designed to calculate the location, although most of the attempts use some type of Artificial Neural Network to address this task, there are other approaches that have been proposed. The study in [2] uses fuzzy logic to get an estimation of the fault section prior to the exact distance calculation using traveling waves. This algorithm claims to work even in a distribution system with the presence of DGs. Other approaches, as in [13], use an MLP with first scale DWT coefficients. The method proposed for a transmission line in [14] applies a special type of ANN, called Extreme Learning Machine (ELM), to perform fault location. The input of the method is just the current waveform for one cycle. This neural network inherently integrates wavelet and gaussian activation functions, which makes it extremely powerful for feature extraction.

As a summary, the aforementioned projects already obtain a high accuracy for fault detection and classification. However, they do not study the increasing relevant area in distribution feeders: the integration of solar PV. The contribution of this paper is to address fault classification under the variability introduced by PV systems.

3. Proposed method

3.1. Description of the problem

The goal of this paper is to develop a method capable of detecting a fault, either if it has been produced on a node with solar PV or not, and infer the fault scenario (i.e., the fault type and location). Measuring devices located across the system will be trained to perform this classification. In practice, each device will be able to independently protect their area of influence. Techniques such as Continuous Wavelet Transform (CWT) are used to analyze the fault signal, and Convolutional Neural Networks are trained to perform the classification of the faulty node and type.

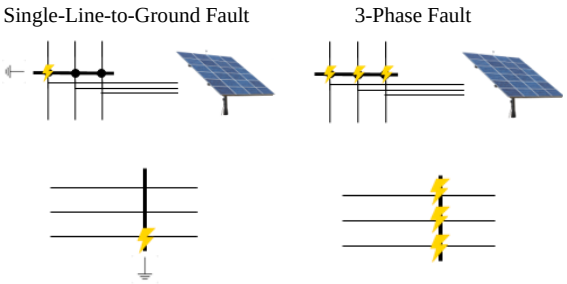

Figure 1. Simulated faults for nodes with and without PV systems

As shown in Figure 1, two types of faults are taken into consideration in this paper: Single-Line-to-Ground (SLG) faults, which are the most common type of faults according to [1], and Three-Phase (3P) faults, which are the most severe types of faults.

Faults are simulated at some of the nodes of the designated test system and the measurements taken by some devices located across the system are analyzed to check the existence of a fault. One of the desirable features of fault detection is speed. Thus, a measurement sampling frequency of 10 MHz is used, and the data is processed every 0.1 millisecond (every 1000 samples). Such a small period of time implies that the decision of whether a fault has occurred or not will not be based on the whole fault transient, but rather it will be based only on the first part of the fault dynamics: the traveling waves.

3.2. Test system

The system selected to perform the fault simulations is the IEEE 34 node case, which is available in PSCAD format [15]. The simulations were performed with this software tool using the Automation Library for Python.

The system is illustrated in Figure 2, which presents the circuit topology, and main devices, as well as location of PV system and faults (whose location is to be detected). The system has the following features:

- 34 nodes (node 800 corresponds to the substation).
- 9 fault locations, which are located in nodes: 806, 812, 820, 824, 830, 856, 888, 846 and 836.
- 3 PV systems on nodes: 812, 836 and 846.
- 5 measuring devices that record 3-phase current at a sampling frequency of 10 MHz. These devices are located in nodes: 800, 850, 828, 832 and 860.

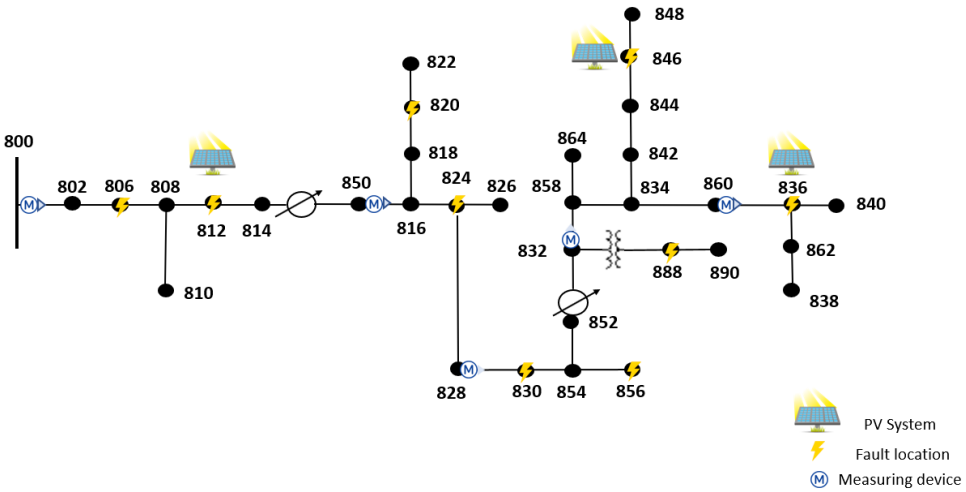

Figure 2. Test system

The distribution lines of the circuit have been modeled in a way that the frequency-dependent (phase) model available on PSCAD can be used for performing the simulations. The usage of this model is of special importance in order to obtain an accurate representation of the traveling waves, as the propagation of each of its frequency components depends on the line characteristics. More information about the utilized line modeling is available in [16] and [17].

3.3. Solar PV system

The solar farm model was obtained from PSCAD and it is used to represent the PV systems. The inputs to this model are:

- Irradiance. Two values: 600 and 1000 W/m^2 are employed for the simulations.
- Temperature. Two values: 28 and 50°C are employed for the simulations.
- Output power reference, which is set to 200 kW (2 units of 100 kW each).
- Output voltage reference, which is set to 24.9 kV (1 p.u. in terms of the voltage base).

3.4. Continuous Wavelet Transform

The Continuous Wavelet Transform (CWT) is a powerful signal processing tool that is used to analyze the frequency components of a signal along a period of time. In this transform, the signal is split into frequency components, which are evaluated for different scales. This method can provide high-frequency resolution for low scales, which is needed to determine the arrival time of the traveling wave.

The mother wavelet ψ(t), which in this case is the Morlet wavelet, is scaled by the scale coefficient a and translated by the translation coefficient b. The CWT of the signal x(t) is then defined by [10]:

$$CWT_x(a,b) = \frac{1}{\sqrt{a}} \int_{-\infty}^{\infty} x(t)\, \psi\left(\frac{t-b}{a}\right) \mathrm{dt} \qquad (1)$$

The result of the transformation is a rectangular matrix in which the number of rows is equal to the number of scales and the number of columns is equal to the number of samples. Each scale is related with a frequency. Applying the conversion to the scales, it is possible to obtain a representation of the frequency components along time. Each column represents the frequency spectrum of the wave at each instant of time.

3.5. Algorithm

An overview of the workflow to compose the training set is illustrated in Figure 3. The first stage corresponds to the simulation of faults in the system. The system is assumed to be in steady state. Each fault is simulated individually at each location using the following characteristics:

- Fault resistance values: 0.01, 0.1, 1.0 and 10 Ω.
- Fault type: 3-phase and single-line-to-ground (SLG) fault were simulated for the 3-phase nodes. SLG faults have been simulated for the single-phase nodes.

Taking in account all the different locations, types of faults, resistance values, and the various combinations of irradiance and temperature values, the number of simulated faults is 256. For each multimeter, the recorded current waveform is processed in several steps: First, the measurements are divided into slices of 0.1 ms (non-overlapping) to resemble the operation of the protection device. Second, the 3-phase current measurements are decoupled using the Karrenbauer transformation [18] into 3 independent modes: the ground mode and two aerial modes. The CWT was applied to the ground mode for each slice.

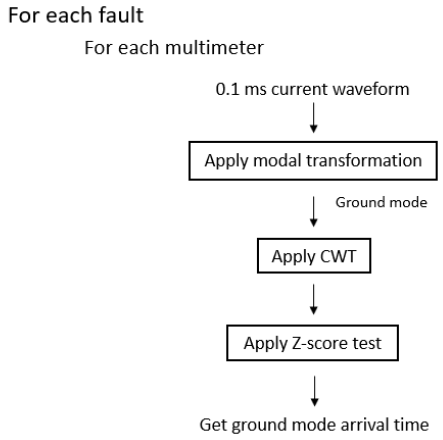

Figure 3. Workflow of the algorithm

The first scale coefficients, which are related with the highest frequencies of the wave, are used to identify the maximum modulus wavelet coefficient in each one of the 0.1 ms timeframes. Actually, each slice has a maximum modulus coefficient, but the traveling wave arrival is only noticed by a sudden and large change of magnitude between two consecutive 0.1 ms windows. A statistical analysis based on the Z-score test is employed to determine if a fault has been detected (a given data point is too far from the given distribution of points). According to the Z-score test, when a point is more than

3 standard deviations away from the average, it is considered as an outlier. For each new data point, it is calculated whether if it is an outlier or not. If the answer is positive, a fault has been detected. If not, the average and the standard deviation are recalculated using this new data.

Once the fault is detected, the arrival time of the ground mode is given by the location of the maximum modulus coefficient in its time slice. This way, the arrival time for all the multimeters is obtained, but only the recorded wave of the multimeter with the lowest arrival time will be used for training purposes. This approach enforces the idea that each multimeter will be in charge of some nodes around it, as it would be the first one in detecting a fault inside its area of influence.

In order to have a common benchmark for the training process, the current waveform of the selected multimeter is cropped 0.5 ms before and after the ground mode arrival time, and the CWT of that 1 ms window is saved for the training of the CNN. It is important to notice that even though the signals are analyzed every 0.1 ms, a little bit more of data is gathered before performing the final CWT. This allows getting a more complete representation of the traveling wave, which helps in the classification task. Given that simulated faults are labelled, a supervised algorithm is going to be used for the training process. Otherwise, it could be difficult to address which patterns in the data actually refer to changes in location or type and which patterns are due to other conditions, such as resistance, irradiance, etc. For this project, a Convolutional Neural Network is the chosen algorithm for its suitability and superior performance in image classification. In practice, the CWT matrices can be treated as images. One CNN is trained for node classification, and another one for type classification.

Only 192 of the 256 matrices of coefficients that compose the training set are used to train the CNNs. The remaining 64 matrices are used for the test set. The size of each matrix is 104-by-10000, where 104 is the number of scales and 10000 the number of samples that is obtained in 1 ms at 10 MHz. However, in order to reduce the required computation effort and the resources needed to train both CNNs, a down-sampling with a factor of 100 was used in order to reduce the size of the obtained CWT coefficient matrices. Therefore, the training set is composed by matrices of size 104-by-100.

As mentioned before, the first CNN is trained to infer the node of the fault, while the second one predicts the type. The structure of first neural network is summarized in Table I, while the structure of second neural network is summarized in Table II. For the first neural network, the dense layer has 9 neurons that represents all the possible locations of the fault. It will give the probability for each node. The dense layer of the second neural network has 2 neurons and it will return the probability of each of the fault type, SLG and 3-Phase.

Table I. Configuration of each layer in the CNN for fault node

Layer type	Kernel size	Output size
Convolutional	5x5	100x96x104
Max Pooling	-	50x48x104
Convolutional	3x3	48x46x52
Dropout	-	48x46x52
Convolutional	2x2	47x45x26
Average Pooling	-	23x22x26
Flatten	-	13156
Dense	-	9

Table II. Configuration of each layer in the CNN for fault type

Layer type	Kernel size	Output size
Convolutional	5x5	100x96x104
Max Pooling	-	50x48x104
Convolutional	4x4	47x45x52
Average Pooling	-	23x22x52
Convolutional	3x3	21x20x26
Average Pooling	-	10x10x26
Flatten	-	2600
Dense	-	2

4. Results

The intermediate results obtained from the fault detection procedure and the results from the classification tasks using Convolutional Neural Networks are shown in this section. Both CNNs are trained for all the fault scenarios at the same time. This way, all the multimeters are trained to detect all the faults. In this particular case, this approach enhances the training process as a larger number of samples can be used for learning. However, for a larger system, it is important to notice that it would be optimal to train a model for each multimeter with just the fault signals that can be observed in its area of influence.

4.1. Detection of the fault

As it was mentioned in Section III, the ground mode is used for fault detection. The signal is divided into 0.1 ms slices and then CWT is applied to each slice. Then,

the magnitude and location of the maximum modulus coefficient is recorded. A statistical analysis based on the Z-score test is employed to detect the arrival of traveling wave caused by a fault, which is noticed by a sudden increase in the maximum recorded magnitude between two consecutive periods.

Figure 4 illustrates the method. The traveling wave arrives when time is approximately 1.1ms. Before the arrival, the maximum recorded magnitude of each 0.1 ms period remains quite constant and low. However, the presence of high frequency components makes the signal much more diverse and the magnitudes of the coefficients become higher. In the figure, the points illustrate the maximum modulus coefficients in each time window and are plotted at the instant of time when they occurred.

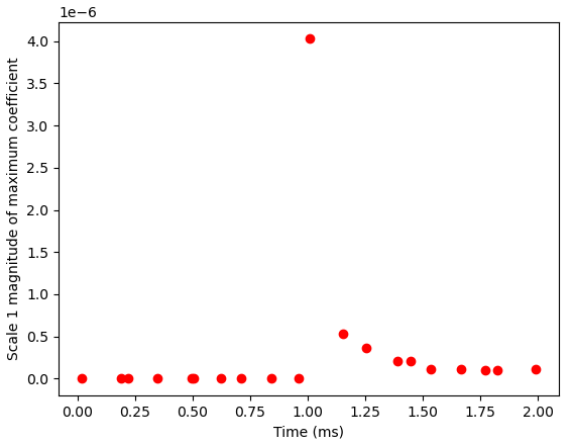

Figure 4. Magnitudes and index of the maximum modulus CWT coefficients before and after a fault event

Once a fault has been detected, the current signal for the winner measuring device is cropped 0.5 ms before and after the traveling wave ground mode arrival time. As mentioned before, this allows the algorithm to gather more information from the traveling wave. In Figure 5, two of these fault signals can be appreciated. The faults were simulated in the same location (node 812, where a PV is located), for the same resistance value (1 ohm) and for the same irradiance (600 W/m^2) and temperature conditions (28°C). The only difference is the type of fault: one is SLG and the other one is 3-P. It is noticed that traveling waves of 3-phase faults show oscillations around zero, while SLG faults usually shows a large increase of current with respect to the pre-fault conditions. This characteristic behavior is observed in other faults as well.

A)

B)

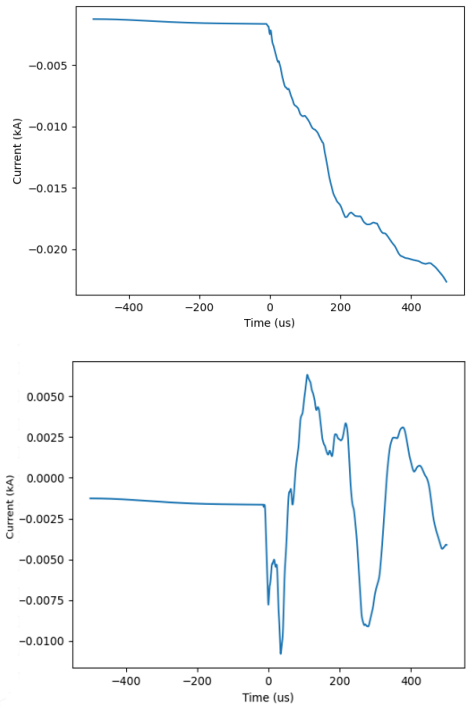

Figure 5. A) SLG fault B) 3-Phase fault. Cropped current waveform

4.2. Continuous Wavelet Transform

The CWT is then applied to the 1 ms cropped signal. Each matrix of coefficients is distinct for each fault location, type, and resistance value. Irradiance and temperature conditions on the PV systems include variation as well. Therefore, these matrices are suitable for fault classification. In Figure 6, the CWT coefficients for different types of faults are shown. The size of each matrix is 104-by-100 and they can be interpreted as images. The CNNs are then trained to extract and learn the features of each image.

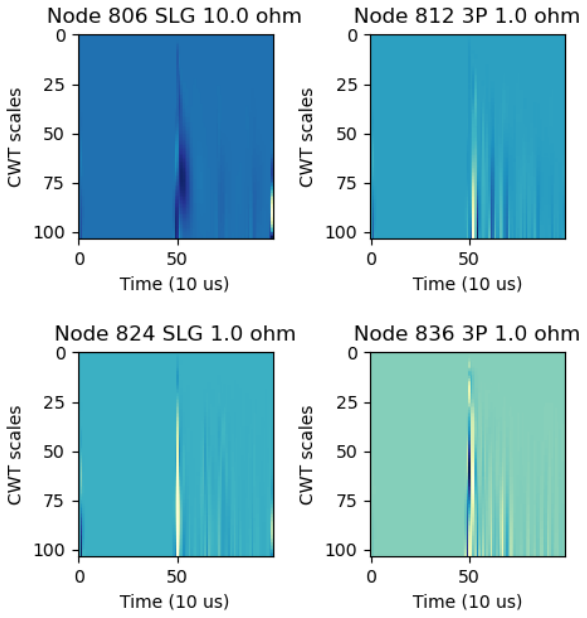

Figure 6. CWT coefficient matrices for four of the simulated faults

4.3. Testing

The test set is composed by faults for nodes with and without PV systems. In total, 64 cases are studied. The CWT coefficients matrices correspond to combinations of resistance values, irradiance or temperature that had not been shown during the model training stage. For the location of the faulty node, the accuracy of the prediction is 89.06%. This result is comparable with the one obtained in [2] for the fault section detection algorithm, where the accuracy is 100% but the number of locations is only 4. In [10], for a simpler test system, the accuracy for detecting the faulty feeder is around 99%. Considering the complexity regarding the number of locations and the scale of the system, the obtained results can be considered as satisfactory. For the type classification, the accuracy is 87.5%.

Figure 7 summarizes the results of the node location prediction. For 7 out of the 9 tested nodes, the CNN correctly guesses the real node. This may be related with the small size of the system: as the number of nodes is reduced and they are not spatially close to each other, fault signals are quite distinct and classification becomes easier. Furthermore, it can be stated that the CNN successfully addresses in those cases the variability introduced by different resistance values and irradiance and temperature conditions. Results are not so satisfactory for node 820, where one of the predictions is not accurate, and for node 888, where most of the predictions point out node 846 although the faults were not produced there. However, except in those two particular cases, the CNN model seems to have a great overall accuracy.

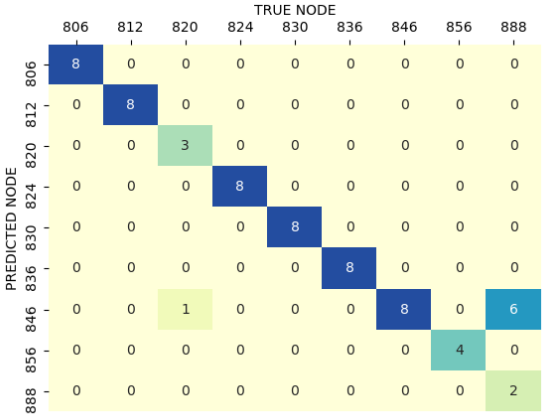

Figure 7. Confusion matrix for node prediction

As shown in Figure 8. it is remarkable to see that all the SLG faults are predicted correctly. However, some 3P faults (on nodes 846 and 888) are not classified correctly.

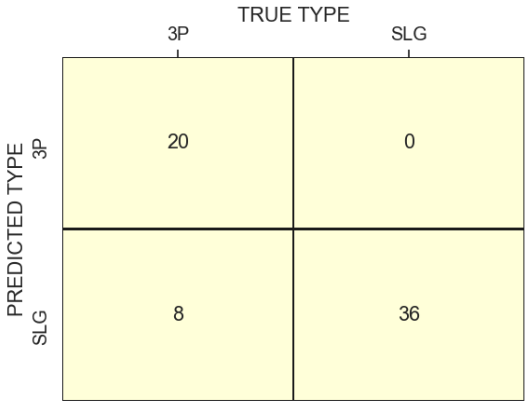

Figure 8. Confusion matrix for type prediction

5. Future work

As it is the first paper of this project, the number of simulated faults was limited to 256. While the classification results are satisfactory for the amount of simulated data, a further expansion of the project could involve more combinations of fault locations and resistance values. Furthermore, a deeper analysis of this system would need to test robustness of the system against high-impedance faults. These faults pose a large threat on distribution systems as fault currents tend to be very low and, therefore, difficult to detect.

In addition, the algorithm could be trained with other waveforms that include high-frequency components but are not produced by fault events. This would allow the measuring device to distinguish faults from other events such as capacitor turning on and off or regulator taps switching.

The results obtained in this paper suggest that this approach could be a promising fault classification method for a real system. However, further research regarding noisy measurements, different inception angles and actual processing times on a device should be conducted.

6. Conclusion

This paper addresses the task of fault classification (node location and fault type) for a distribution system with high penetration of PV. The simulated fault events include different combinations of irradiance and temperature for the PV systems and different fault resistances.

The first stage of the proposed method is the detection of the fault event. In order to perform a fast detection, the algorithm infers the presence of a fault by the detection of the produced traveling wave. The CWT is employed to analyze the signal. Any change in the signal frequency components will be reflected on the CWT coefficient matrices.

The second step is to use the CWT coefficient matrices of the traveling waves to train two Convolutional Neural Networks to predict both the fault node and the type of the fault. The results suggest that the CNN is a promising tool able to extract features from the matrices, which leads to a great performance in fault classification. Results shows that node prediction accuracy is 89.06%, while fault type prediction reaches up to 87.5%.

7. Acknowledgements

This research was partially funded by Sandia National Laboratories.

Sandia National Laboratories is a multimission laboratory managed and operated by National Technology & Engineering Solutions of Sandia, LLC, a wholly owned subsidiary of Honeywell International Inc., for the U.S. Department of Energy's National Nuclear Security Administration under contract DE-NA0003525.

8. References

[1] S. S. Gururajapathy, H. Mokhlis and H. A. Illias. "Fault location and detection techniques in power distribution systems with distributed generation: A review," in Renewable and Sustainable Energy Reviews, Elsevier, vol. 74(C), pages 949-958, 2017.

[2] Xu Chen, Xianggen Yin, Shanfei Deng. "A Novel Method for SLG Fault Location in Power Distribution System Using Time Lag of Travelling Wave Components", in Transactions of Electrical and Electronic Engineering, Institute of Electrical Engineers of Japan, vol. 12, issue 1, pp. 45-54, 2017.

[3] Eyada A. Alanzi, Mahmoud A. Younis, Azrul Mohd Ariffin, "Detection of faulted phase type in distribution systems based on one end voltage measurement", in International Journal of Electrical Power & Energy Systems, vol. 54, pp. 288-292, 2014.

[4] F. V. Lopes, K. M. Dantas, K. M. Silva and F. B. Costa, "Accurate Two-Terminal Transmission Line Fault Location Using Traveling Waves," in IEEE Transactions on Power Delivery, vol. 33, no. 2, pp. 873-880, April 2018.

[5] A. Borghetti, M. Bosetti, M. Di Silvestro, C. A. Nucci and M. Paolone, "Continuous-Wavelet Transform for Fault Location in Distribution Power Networks: Definition of Mother Wavelets Inferred From Fault Originated Transients," in IEEE Transactions on Power Systems, vol. 23, no. 2, pp. 380-388, May 2008.

[6] A. Borghetti, M. Bosetti, C. A. Nucci, M. Paolone and A. Abur, "Integrated Use of Time-Frequency Wavelet Decompositions for Fault Location in Distribution Networks: Theory and Experimental Validation," in IEEE Transactions on Power Delivery, vol. 25, no. 4, pp. 3139-3146, Oct. 2010.

[7] M. Jamil, R. Singh & S. Sharma. "Fault Identification In Electrical Power Distribution System Using Combined Discrete Wavelet Transform and Fuzzy Logic," in Journal of Electrical Systems and Information Technology, vol.2, 2015.

[8] H. Livani and C. Y. Evrenosoğlu, "A Fault Classification and Localization Method for Three-Terminal Circuits Using Machine Learning," in IEEE Transactions on Power Delivery, vol. 28, no. 4, pp. 2282-2290, Oct. 2013.

[9] J. Gracia, A. J. Mazon and I. Zamora, "Best ANN structures for fault location in single-and double-circuit transmission lines," in IEEE Transactions on Power Delivery, vol. 20, no. 4, pp. 2389-2395, Oct. 2005.

[10] M. Guo, X. Zeng, D. Chen and N. Yang, "Deep-Learning-Based Earth Fault Detection Using Continuous Wavelet Transform and Convolutional Neural Network in Resonant Grounding Distribution Systems," in IEEE Sensors Journal, vol. 18, no. 3, pp. 1291-1300, Feb. 2018.

[11] S. Lan, M. Chen and D. Chen. "A Novel HVDC Double-Terminal Non-Synchronous Fault Location Method Based on Convolutional Neural Network," in IEEE Transactions on Power Delivery, 2019.

[12] J. Liang, T. Jing, H. Niu and J. Wang, "Two-Terminal Fault Location Method of Distribution Network Based on Adaptive Convolution Neural Network," in IEEE Access, vol. 8, pp. 54035-54043, 2020.

[13] M. N. Hashim, M. K. Osman, M. N. Ibrahim, A. F. Abidin and M. N. Mahmud, "Single-ended fault location for transmission lines using traveling wave and multilayer perceptron network," 2016 6th IEEE International Conference on Control System, Computing and Engineering (ICCSCE), Batu Ferringhi, 2016, pp. 522-527.

[14] Y. Q. Chen, O. Fink and G. Sansavini. "Combined Fault Location and Classification for Power Transmission Lines Fault Diagnosis With Integrated Feature Extraction," in IEEE Transactions on Industrial Electronics, vol. 65, pp. 561-561, 2018.

[15] PSCAD Q&A, IEEE 34 bus example. Available at: https://forum.hvdc.ca/833005/IEEE-34-bus-example

[16] Distribution System Analysis Subcommittee. Radial Distribution Test Feeders.

[17] Distribution System Analysis Subcommittee. IEEE 34 Node Test Feeder.

[18] H. Jia. "An Improved Traveling-Wave-Based Fault Location Method with Compensating the Dispersion Effect of Traveling Wave in Wavelet Domain," in Mathematical Problems in Engineering, 2017.